

# Investigation of the millisecond pulsar origins by their spin periods at the wavebands of radio, X-ray and $\gamma$ -ray

De-Hua Wang • Cheng-Min Zhang •  
Shuang-Qiang Wang

**Abstract** To track the formation and evolution links of the millisecond pulsars (MSPs) powered by accretion and rotation in the galactic field, we investigate the spin period ( $P$ ) and spin-down power ( $\dot{E}$ ) distributions of the MSPs observed at the wavebands of radio, X-ray and  $\gamma$ -ray. We find that all but one (119/120) of the  $\gamma$ -ray MSPs have been detected with the radio signals (radio+ $\gamma$  MSPs), on the contrary, nearly half of the radio MSPs (118/237) have not been detected with  $\gamma$ -rays (radio-only MSPs). In addition, the radio+ $\gamma$  MSPs are shown to be the relative faster and more energetic objects ( $\langle P \rangle \sim 3.28$  ms and  $\langle \dot{E} \rangle \sim 4.5 \times 10^{34}$  erg s $^{-1}$ ) compared with the radio-only MSPs ( $\langle P \rangle \sim 4.70$  ms and  $\langle \dot{E} \rangle \sim 1.0 \times 10^{34}$  erg s $^{-1}$ ), **while the spin periods of these two MSP populations are compatible with the log-normal distributions by the statistical tests.** Most rotation-powered MSPs (RMSPs) with the radio eclipsing (31/34) exhibit the radio+ $\gamma$  signals, which share the faster spin ( $\langle P \rangle \sim 2.78$  ms) and larger spin-down power ( $\langle \dot{E} \rangle \sim 4.1 \times 10^{34}$  erg s $^{-1}$ ) distributions than the non-eclipsing ones ( $\langle P \rangle \sim 4.19$  ms,  $\langle \dot{E} \rangle \sim 2.4 \times 10^{34}$  erg s $^{-1}$ ), implying the radio+ $\gamma$  MSPs to be younger than the radio-only MSPs. It is no-

ticed that the spin distribution of the accretion-powered X-ray MSPs shows a clustering phenomenon around  $\sim 1.6 - 2.0$  ms, which is not observed in RMSPs, hinting that the RMSPs may experience the multiple possible origins. Particularly, all the three super-fast spinning RMSPs with  $P \sim 1.4 - 1.6$  ms exhibit the non-eclipsing, and we argue that they may be the distinctive sources formed by the accretion induced collapse (AIC) of white dwarfs.

**Keywords** pulsars: general-stars: neutron-gamma rays: stars-X-rays: binaries-accretion, accretion disks

## 1 Introduction

Based on the recycling interpretation for the formation of the millisecond pulsars (MSPs) (Alpar et al. 1982; Radhakrishnan & Srinivasan 1982; Bhattacharya & van den Heuvel 1991), the neutron star (NS) in a low-mass X-ray binary (LMXB) can accrete  $\sim 0.1 - 0.2 M_{\odot}$  (Zhang et al. 2011; Pan et al. 2015) from its companion through the accretion disk during the  $\sim 0.1 - 10$  Gyr (Tauris 2012), then it is spun-up to a spin period of a few milliseconds, and probably also reduce its magnetic field strength to  $\sim 10^7 - 10^9$  G (Bhattacharya & Srinivasan 1995; Zhang & Kojima 2006; Zhang 2016). The overall torque acting onto the NS during the spin up state depends on the disk structure, as well as the interaction between the NS magnetic field and the accretion plasma (Ghosh & Lamb 1979; Ghosh 2007; Kluźniak et al. 2007). After the X-ray accretion phase, the recycled pulsar will change from the accretion-powered X-ray MSP into a rotation-powered MSP (RMSP) by emitting radio pulsation (Lorimer 2008).

Since 1990's, several observational evidence have been found to support the recycling scenario of MSP formation: (1). The first evidence that constructs the

De-Hua Wang

School of Physics and Electronic Science, Guizhou Normal University, Guiyang, 550001, China

Cheng-Min Zhang

<sup>1</sup>National Astronomical Observatories, Chinese Academy of Sciences, Beijing, 100101, China

<sup>2</sup>School of Physical Sciences, The University of Chinese Academy of Sciences, Beijing 101400, China

<sup>3</sup>CAS Key Laboratory of FAST, Chinese Academy of Sciences, Beijing 100101, China

<sup>4</sup>Key Laboratory of Radio astronomy, Chinese Academy of Sciences, Beijing 100101, China

Shuang-Qiang Wang

Xinjiang Astronomical Observatory, Chinese Academy of Sciences, Urumqi, 830011, China

**Table 1** Accretion-powered X-ray MSPs and transitional MSPs in the galactic field.

#	Source	$\nu_s$ (Hz)	$P$ (ms)	Type <sup>§</sup>
AMXP and NMXP in the galactic field				
[1]	IGR J17602-6143	164	6.10	A
[2]	SWIFT J1756.9-2508	182	5.49	A
[3]	XTE J0929-314	185	5.41	A
[4]	XTE J1807.4-294	191	5.24	A
[5]	IGR J17511-3057	245	4.08	A, N
[6]	4U 1916-05	270	3.70	N
[7]	IGR J17191-2821	294	3.40	N
[8]	XTE J1814-338	314	3.18	A, N
[9]	4U 1702-429	330	3.03	N
[10]	4U 1728-34	363	2.75	N
[11]	HETE J1900.1-2455	377	2.65	A, N
[12]	SAX J1808.4-3658	401	2.49	A, N
[13]	IGR J17498-2921	401	2.49	A, N
[14]	4U 0614+09	415	2.41	N
[15]	XTE J1751-305	435	2.30	A
[16]	Swift J1749.4-2807	518	1.93	A
[17]	KS 1731-260	524	1.91	N
[18]	<b>IGR J17591-2342</b>	<b>527</b>	<b>1.90</b>	<b>A</b>
[19]	A 1744-361	530	1.89	N
[20]	<b>SAX J1810.8-2609</b>	<b>532</b>	<b>1.88</b>	<b>N</b>
[21]	Aql X-1 (1908+005)	550	1.82	A, N
[22]	EXO 0748-676	552	1.81	N
[23]	MXB 1659-298	567	1.76	N
[24]	4U 1636-53	581	1.72	N
[25]	MXB 1743-29	589	1.70	N
[26]	IGR J00291+5934	599	1.67	A
[27]	SAX J1750.8-2900	601	1.67	N
[28]	GS 1826-238	611	1.64	N
[29]	4U 1608-52	619	1.62	N
tMSP in the galactic field				
[1]	PSR J1023+0038	592	1.69	
[2]	PSR J1227-4853	593	1.69	

<sup>§</sup> A—accreting millisecond X-ray pulsar;

N—nuclear-powered millisecond X-ray pulsar.

link between the accreting millisecond X-ray pulsar (AMXP, e.g., SAX J1808.4-3658) in LMXB and RMSP was detected by Wijnands & van der Klis (1998), however, it is suggested that some AMXPs may show the transition to the rotation-powered state during the X-ray quiescence (Burderi et al. 2006, 2009; Di Salvo et al. 2008; Hartman et al. 2008, 2009; Sanna et al. 2017). (2). The transition between the accretion- and rotation-powered behaviors have been observed from IGR J18245-2452 (Papitto et al. 2013; Pallanca et al. 2013; Ferrigno et al. 2014; Linares et al. 2014), PSR J1023+0038 (Archibald et al. 2009; Stappers et al. 2014; Patruno et al. 2014), and XSS J12270-4859 (Bassa et al. 2014; Papitto et al. 2014; Roy et al. 2014; Bogdanov et al. 2014) (i.e., the transitional MPSs, or tMSPs, see Papitto 2016). (3). The irregular radio eclipses are observed in some binary RMSPs (i.e., the eclipsing RMSPs including black widows and redbacks, see Roberts 2013; Torres et al. 2017), which are explained as the absorptions by the lost matter ejected from the companions (Fruchter et al. 1988; Kluźniak et al. 1988).

Until now, there have been  $\geq 300$  RMSPs detected (isolated and binary, see the ATNF pulsar catalogue Manchester et al. 2005), where the fastest one, i.e., PSR J1748-2446ad in the globular cluster, shows the spin frequency of 716 Hz (Hessels et al. 2006). While,  $> 30$  **accretion-powered X-ray MSPs** (Patruno et al. 2017) have been detected, including the AMXPs with the spin signals observed from the accretion-powered coherent pulsations (Wijnands & van der Klis 1998; Patruno et al. 2012), and the nuclear-powered millisecond X-ray pulsars (NMXPs) with the spin signals inferred from the thermonuclear burst oscillations (Strohmayer et al. 1996; Chakrabarty et al. 2003; Strohmayer & Bildsten 2006; Watts 2012). The details of the AMXPs, NMXPs and tMSPs in the galactic field are shown in Table 1, **including two new detected sources, i.e., IGR J17591-2342 (Ferrigno et al. 2018; Sanna et al. 2018) and SAX J1810.8-2609 (Bilous et al. 2018)**. Papitto et al. (2014) analyzed the spin distributions of AMXPs, NMSPs, eclipsing and non-eclipsing RMSPs, and find that NMXPs show the significantly faster spins than the most rotation-powered sources, while the eclipsing RMSPs show the faster spins than the non-eclipsing ones. Furthermore, Patruno et al. (2017) indicated that there may exist two sub-populations in the spin frequency distributions of the AMXPs+NMXPs with the mean values of  $\approx 300$  Hz and  $\approx 575$  Hz, respectively.

In the times of *Fermi* satellite, there are more than 100 MSPs detected with  $\gamma$ -ray signals (from  $\sim 20$  MeV to over 300 GeV, see Abdo et al. 2013), and these  $\gamma$ -ray MSPs tend to be the shorter-period, more energetic population than the canonical, non-recycled

**Table 2** The MSP samples in the galactic field.

Category	Count	Sub-count	Sub-sub-count	Fraction	Description
LMXBs	<b>29</b>				All accretion-powered X-ray pulsars (AMXPs + NMXPs)
AMXPs		<b>14</b>		48%	Accreting millisecond X-ray pulsars
NMXPs		<b>21</b>		<b>72%</b>	Nuclear-powered millisecond X-ray pulsars
RMSPs	237				Rotation-powered (radio) millisecond pulsars
eclipsing RMSPs		34		14%	RMSPs with irregularly eclipses in radio-pulsed emission
radio+ $\gamma$ MSPs			31	13%	Eclipsing RMSPs detected with both radio and $\gamma$ -ray signals
radio-only MSPs			3	1%	Eclipsing RMSPs detected with radio but without $\gamma$ -ray signals
non-eclipsing RMSPs		203		86%	RMSPs whose radio-pulsed emission is not be eclipsed
radio+ $\gamma$ MSPs			88	37%	Non-eclipsing RMSP detected with both radio and $\gamma$ -ray signals
radio-only MSPs			115	49%	Non-eclipsing RMSP detected with radio but without $\gamma$ -ray signals
radio-quiet $\gamma$ -ray MSPs	1			100%	The MSP is detected with $\gamma$ -ray signal but without radio signal

ones (Ray et al. 2012; Abdo et al. 2013; Caraveo 2014; Grenier & Harding 2015). Motivated by the analysis on the spin distributions of the MSPs by Papitto et al. (2014) and Patruno et al. (2017), as well as the  $\gamma$ -ray observations for RMSPs, we try to compare the distributions of the spin period ( $P$ ) and spin-down power ( $\dot{E}$ ) of various MSPs at the different wavebands and powered by the accretion or spin-down, by which we may infer their origins, e.g., recycling process or accretion induced collapse (AIC) of white dwarf process.

The structure of the paper is organized as follows. In Section 2, we introduce the population of MSPs. Then in Section 3, we compare the  $P$  and  $\dot{E}$  distributions between the MSP samples with the different wavebands, e.g., radio, X-ray and  $\gamma$ -ray. Finally, we present the discussions and conclusions in Section 4.

## 2 Population of millisecond pulsars

We follow the work by Papitto et al. (2014) and Patruno et al. (2017) to collect the MSP samples, including the accretion-powered X-ray MSPs (AMXPs+NMXPs), eclipsing and non-eclipsing RMSPs. However, this paper focuses on the comparisons of MSPs at various radiation wavebands: AMXPs and NMXPs—X-ray, eclipsing and non-eclipsing RMSPs—radio or  $\gamma$ -ray. In addition, the selections of the MSP samples are also constrained by the following rules: (1). Only the MSPs in the galactic field are taken into account, while the ones in the globular cluster are excluded because they may undergo the more complicated evolution processes. (2). The MSP samples are selected with  $P < 10$  ms, as it includes most of the observed  $\gamma$ -ray MSPs. (3). Both the isolated and binary RMSPs are considered, since the progenitors of the isolated RMSPs must have gone through episodes of accretion (recycling) in their past history (Patruno et al. 2017). (4) Papitto et al. (2014) consider the "transitional MSPs" as the combination of AMXPs and eclipsing RMSPs, here instead, we follow

Patruno et al. (2017) and refer the transitional MSPs in the galactic field as the two systems shown in Table 1, for which there is actual evidence of a transition.

The details of the collected MSP samples are summarized in Table 2, where the accretion-powered X-ray MSPs are referred to Papitto et al. (2014) and Patruno et al. (2017), the RMSPs are referred to the catalogs compiled by ATNF<sup>1</sup> (Manchester et al. 2005) and D. R. Lorimer<sup>2</sup>, the  $\gamma$ -ray MSPs are referred to D. R. Lorimer<sup>3</sup> and "Public List of LAT-Detected Gamma-Ray Pulsars"<sup>3</sup>, and the eclipsing RMSPs are referred to "Millisecond Pulsar Catalogue"<sup>4</sup>. It is noticed that all but one of the  $\gamma$ -ray MSPs (119/120) have been detected with the radio signals, which are recorded as radio+ $\gamma$  MSPs, on the contrary, nearly half of the radio MSPs (118/237) have not been detected with the  $\gamma$ -ray signals, which are recorded as radio-only MSPs. Besides, most eclipsing RMSPs (31/34) show radio+ $\gamma$  signals, and two tMSPs in the galactic field (both are eclipsing RMSPs), i.e., PSR J1023+0038 and PSR J1227-4853, have shown the transition from the X-ray emission in the accretion-powered stage to the radio emission in the rotation-powered stage, where PSR J1227-4853 has also been detected with  $\gamma$ -ray pulsation in the rotation-powered stage. There is only one MSP (PSR J1744-7619) that has been detected with  $\gamma$ -ray signal but without radio signal ( $< 30 \mu\text{Jy}$ , see Abdo et al. 2013), i.e., the radio-quiet  $\gamma$ -ray MSP, which shows the spin period of  $\sim 4.7$  ms (Clark et al. 2018).

<sup>1</sup><http://www.atnf.csiro.au/research/pulsar/psrcat/>

<sup>2</sup><http://astro.phys.wvu.edu/GalacticMSPs/GalacticMSPs.txt>

<sup>3</sup><https://confluence.slac.stanford.edu/display/GLAMCOG/Public+List+of+LAT-Detected+Gamma-Ray+Pulsars>

<sup>4</sup><https://apatruno.wordpress.com/about/millisecond-pulsar-catalogue/>

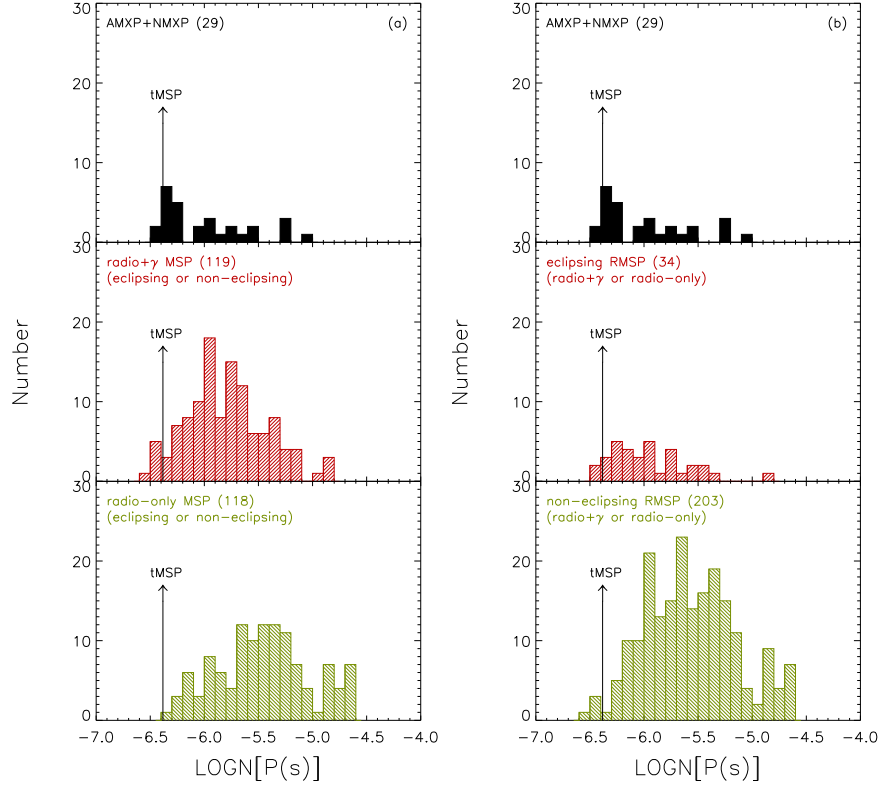


**Fig. 1** Spin period distributions of the MSP samples (**the horizontal axis stands for the natural logarithm of  $P$** ): (a) accretion-powered X-ray MSPs, radio+ $\gamma$  and radio-only MSPs; (b) accretion-powered X-ray MSPs, eclipsing and non-eclipsing RMSPs. The spin periods of the tMSP PSR J1023+0038 ( $P \sim 1.69$  ms) and PSR J1227-4853 ( $P \sim 1.69$  ms) are also indicated in the figures.

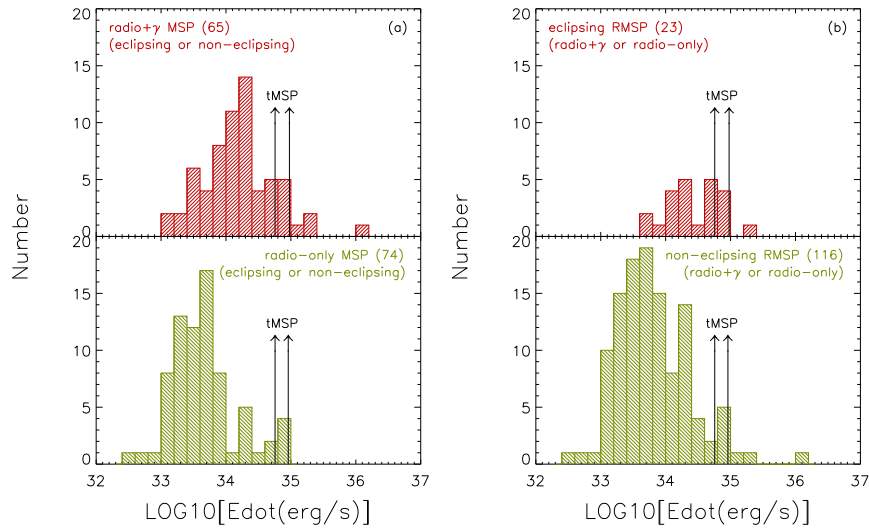


**Fig. 2** Spin-down power distributions of the MSP samples: (a) radio+ $\gamma$  and radio-only MSPs; (b) eclipsing and non-eclipsing RMSPs. The spin-down powers of the tMSP PSR J1023+0038 ( $\dot{E} \sim 5.7 \times 10^{34} \text{ erg s}^{-1}$ ) and PSR J1227-4853 ( $\dot{E} \sim 9.1 \times 10^{34} \text{ erg s}^{-1}$ ) are also indicated in the figures.

**Table 3** Spin period statistics of the MSP samples.

Category	Count	Range	$\langle P \rangle^a$	$\tilde{P}^b$	$\sigma_P^c$
(ms)					
LMXBs	<b>29</b>	1.62 – 6.10	<b>2.75</b>	<b>2.30</b>	<b>1.33</b>
radio+ $\gamma$ MSPs	119	1.41 – 8.12	3.28	2.96	1.34
radio-only MSPs	118	1.69 – 9.90	4.70	4.20	2.05
eclipsing RMSPs	34	1.61 – 7.61	2.78	2.48	1.20
non-eclipsing RMSPs	203	1.41 – 9.90	4.19	3.68	1.88

<sup>a</sup>  $\langle P \rangle$ : mean of  $P$ ;<sup>b</sup>  $\tilde{P}$ : median of  $P$ ;<sup>c</sup>  $\sigma_P$ : standard deviation of  $P$ .**Table 4**  $K - S$  test<sup>a</sup> results of the spin period and spin-down power distributions.

Category	Count	$K - S$ ( $p$ -value)	Reject $H_0$
<b>Spin Period (<math>P</math>)</b>			
LMXBs	<b>29</b>	<b><math>2.02 \times 10^{-3}</math></b>	yes
radio+ $\gamma$ MSPs	119		
LMXBs	<b>29</b>	<b><math>1.87 \times 10^{-6}</math></b>	yes
radio-only MSPs	118		
radio+ $\gamma$ MSPs	119	<b><math>5.34 \times 10^{-9}</math></b>	yes
radio-only MSPs	118		
<b>Spin-down Power (<math>\dot{E}</math>)</b>			
radio+ $\gamma$ MSPs	<b>65</b>	<b><math>1.58 \times 10^{-9}</math></b>	yes
radio-only MSPs	<b>74</b>		
eclipsing RMSPs	<b>23</b>	<b><math>5.35 \times 10^{-6}</math></b>	yes
non-eclipsing RMSPs	<b>116</b>		

<sup>a</sup>  $H_0$  is the null hypothesis that the two groups of data are from the same continuous distribution, with the confidence level parameter  $\alpha = 0.05$ .**Table 5**  $S - W$  test<sup>a</sup> results of the spin period distribution.

Category	Count	$S - W$ ( $p$ -value)	Reject $H_0$
<b>Normality</b>			
radio+ $\gamma$ MSPs	119	<b><math>7.63 \times 10^{-8}</math></b>	<b>Yes</b>
radio-only MSPs	118	<b><math>1.76 \times 10^{-6}</math></b>	<b>Yes</b>
<b>Log-Normality</b>			
radio+ $\gamma$ MSPs	119	<b><math>2.51 \times 10^{-1}</math></b>	<b>No</b>
radio-only MSPs	118	<b><math>9.87 \times 10^{-2}</math></b>	<b>No</b>

<sup>a</sup>  $H_0$  is the null hypothesis that the data follows a normal or a log-normal distribution, with the confidence level parameter  $\alpha = 0.05$ .

### 3 Comparison of the $P$ and $\dot{E}$ distributions

We collect  $P$  and  $\dot{E}$  data of the MSP samples, and then compare their distributions among the various MSP categories classified by the wavebands, e.g., radio, X-ray and  $\gamma$ -ray.

#### 3.1 The distribution of $P$

The spin period statistics, including the range, mean ( $\langle P \rangle$ ), median ( $\tilde{P}$ ) and standard deviation ( $\sigma_P$ ), of the various MSP categories are summarized in Table 3, and Figure 1 shows the corresponding histograms. It can be seen that the radio+ $\gamma$  MSPs (total 119) show the  $P$  distribution ( $\langle P \rangle \sim 3.28$  ms and  $\tilde{P} \sim 2.96$  ms) intermediate between the radio-only MSPs (total 118,  $\langle P \rangle \sim 4.70$  ms and  $\tilde{P} \sim 4.20$  ms) and the accretion-powered X-ray MSPs (total **29**,  $\langle P \rangle \sim 2.75$  ms and  $\tilde{P} \sim 2.30$  ms). The *Kolmogorov - Smirnov* ( $K - S$ ) test shows that the spin periods of these three types of MSPs come from the different continuous distribution at the 95 percent confidence level, as shown in Table 4.

We obtain the similar conclusions to those of *Patruno et al. (2017)* that the accretion-powered X-ray MSPs show a clustering phenomenon in the  $P$  distribution around  $\sim 1.6 - 2.0$  ms (the corresponding spin frequency is  $\sim 500 - 600$  Hz, see Figure 1). In addition, it should be also noticed from Table 3 and Figure 1(a) that the radio-only MSPs and the accretion-powered X-ray MSPs show the similar minimal spin periods of  $P \sim 1.6$  ms, however, three radio+ $\gamma$  MSPs show the even faster spins: PSR J0952-0607 ( $P \sim 1.41$  ms, see *Bassa et al. 2017*), PSR J1803+1358 ( $P \sim 1.52$  ms, see the catalog from *D. R. Lorimer*<sup>5</sup>) and PSR J1939+2134 (B1937+21,  $P \sim 1.56$  ms, see *Backer et al. 1982*). Some analysis argued that the spin periods of the RMSPs may be from a population with a log-normal distribution (*Lorimer et al. 2015*), but not with a normal distribution (*Tauris 2012; Papitto et al. 2014*). Here we take the *Shapiro - Wilk* ( $S - W$ ) test to check the  $P$  distributions of the radio+ $\gamma$  and radio-only MSPs, and find that both populations show the spin periods to be incompatible with a normal distribution at the 95 percent confidence level, but compatible with a log-normal distribution with  $(\mu \pm \sigma)_{\text{radio}+\gamma} \sim (-5.79 \pm 0.37) \log_e(s)$  and  $(\mu \pm \sigma)_{\text{radio-only}} \sim (-5.45 \pm 0.43) \log_e(s)$ , respectively (see Table 5).

<sup>5</sup><http://astro.phys.wvu.edu/GalacticMSPs/GalacticMSPs.txt>



**Table 6** Spin-down power statistics of the MSP samples.

Category	Count	Range	$\langle \dot{E} \rangle^a$	$\tilde{\dot{E}}^b$	$\sigma_{\dot{E}}^c$
			( $\text{erg s}^{-1}$ )		
radio+ $\gamma$ MSPs	65	$1.4 \times 10^{33} - 1.1 \times 10^{36}$	$4.5 \times 10^{34}$	$1.5 \times 10^{34}$	$1.4 \times 10^{35}$
radio-only MSPs	74	$2.8 \times 10^{32} - 9.8 \times 10^{34}$	$1.0 \times 10^{34}$	$4.4 \times 10^{33}$	$1.9 \times 10^{34}$
eclipsing RMSPs	23	$5.3 \times 10^{33} - 1.6 \times 10^{35}$	$4.1 \times 10^{34}$	$2.5 \times 10^{34}$	$3.8 \times 10^{34}$
non-eclipsing RMSPs	116	$2.8 \times 10^{32} - 1.1 \times 10^{36}$	$2.4 \times 10^{34}$	$5.3 \times 10^{33}$	$1.0 \times 10^{35}$

<sup>a</sup>  $\langle \dot{E} \rangle$ : mean of  $\dot{E}$ ;

<sup>b</sup>  $\tilde{\dot{E}}$ : median of  $\dot{E}$ ;

<sup>c</sup>  $\sigma_{\dot{E}}$ : standard deviation of  $\dot{E}$ .

Furthermore, the similar results to Papitto et al. (2014) and Patruno et al. (2017) can be obtained from Table 3 and Figure 1(b) that the eclipsing RMSPs (total 34) show the  $P$  distribution ( $\langle P \rangle \sim 2.78$  ms and  $\tilde{P} \sim 2.48$  ms) faster than the non-eclipsing RMSPs (total 203,  $\langle P \rangle \sim 4.19$  ms and  $\tilde{P} \sim 3.68$  ms). It should be also noticed that all the three fastest radio+ $\gamma$  MSPs, i.e., PSR J0952-0607, PSR J1803+1358 and PSR J1939+2134 (B1937+21) have not been reported with the observed radio eclipsing phenomena.

It is convenient to take the two tMSPs in the galactic field, i.e., PSR J1023+0038 and PSR J1227-4853, as a reference to check the  $P$  and  $\dot{E}$  distributions of the MSP samples. Figure 1 shows that their spin periods are same (both  $P \sim 1.69$  ms, see also Table 1), which are faster than the other MSP samples, but slower than the three fastest radio+ $\gamma$  MSPs.

### 3.2 The distribution of $\dot{E}$

The spin-down power statistics, including the range, mean ( $\langle \dot{E} \rangle$ ), median ( $\tilde{\dot{E}}$ ) and standard deviation ( $\sigma_{\dot{E}}$ ), of the various MSP categories are summarized in Table 6, and Figure 2 shows the corresponding histograms.

It can be seen from Table 6, Figure 2(a) and Figure 2(b) that the radio+ $\gamma$  MSPs (total 65) show the  $\dot{E}$  distribution ( $\langle \dot{E} \rangle \sim 4.5 \times 10^{34} \text{ erg s}^{-1}$  and  $\tilde{\dot{E}} \sim 1.5 \times 10^{34} \text{ erg s}^{-1}$ ) larger than the radio-only MSPs (total 74,  $\langle \dot{E} \rangle \sim 1.0 \times 10^{34} \text{ erg s}^{-1}$  and  $\tilde{\dot{E}} \sim 4.4 \times 10^{33} \text{ erg s}^{-1}$ ), while the eclipsing RMSPs (total 23) show the  $\dot{E}$  distribution ( $\langle \dot{E} \rangle \sim 4.1 \times 10^{34} \text{ erg s}^{-1}$  and  $\tilde{\dot{E}} \sim 2.5 \times 10^{34} \text{ erg s}^{-1}$ ) larger than the non-eclipsing RMSPs (total 116,  $\langle \dot{E} \rangle \sim 2.4 \times 10^{34} \text{ erg s}^{-1}$  and  $\tilde{\dot{E}} \sim 5.3 \times 10^{33} \text{ erg s}^{-1}$ ). **The  $K - S$  test indicates that the  $\dot{E}$  of the radio+ $\gamma$  and radio-only MSPs come from the different continuous distributions at the 95 percent confidence level, while the  $\dot{E}$  of the eclipsing and non-eclipsing RMSPs**

**also come from the different continuous distributions, as shown in Table 4.**

The two tMSPs, i.e., PSR J1023+0038 and PSR J1227-4853, show the  $\dot{E}$  of  $\sim 5.7 \times 10^{34} \text{ erg s}^{-1}$  and  $\sim 9.1 \times 10^{34} \text{ erg s}^{-1}$  respectively, which are larger than those of most other MSP samples (see Figure 2). In addition, as expected, the fast rotator PSR J1939+2134 (B1937+21) with  $P \sim 1.56$  ms shows the large  $\dot{E}$  of  $\sim 1.1 \times 10^{36} \text{ erg s}^{-1}$ .

## 4 Discussions and Conclusions

We compare the  $P$  and  $\dot{E}$  distributions among various types of MSPs in the galactic field, including the accretion-powered X-ray MSPs (AMXPs+NMSPs), eclipsing and non-eclipsing RMSPs, and focus on their radiative wavebands. The details of the discussions and conclusions are summarized as below:

- The count of the radio+ $\gamma$  MSPs (119) collected in the paper is comparable to that of the radio-only MSPs (118, see Table 2), and the radio+ $\gamma$  MSPs tend to be the shorter-period ( $\langle P \rangle \sim 3.28$  ms), more energetic ( $\langle \dot{E} \rangle \sim 4.5 \times 10^{34} \text{ erg s}^{-1}$ ) population than the radio-only MSPs ( $\langle P \rangle \sim 4.70$  ms and  $\langle \dot{E} \rangle \sim 1.0 \times 10^{34} \text{ erg s}^{-1}$ , see Table 3, Table 6, Figure 1(a) and Figure 2(a)). Arons (1996) suggests that due to some threshold voltage, the  $\gamma$ -ray luminosity  $L_\gamma$  of the pulsar may relate to  $\dot{E}$  as  $L_\gamma \propto \dot{E}^{1/2}$ , which is basically supported by the observations from *Fermi* (Abdo et al. 2013). For a magnetic dipole model of the pulsar, combining the relations of  $\dot{E} \sim (32\pi^4/3c^3)(B^2R^6/P^4) \propto P^{-4}$  and  $L_\gamma \propto \dot{E}^{1/2}$  will derive  $L_\gamma \propto P^{-2}$ , which may explain why the MSPs with the faster  $P$  or larger  $\dot{E}$  are more likely to emit  $\gamma$ -rays. In fact, all the  $\gamma$ -ray MSP samples in the paper show  $P < 10$  ms and  $\dot{E} > 10^{33} \text{ erg s}^{-1}$ . It is also noticed that most eclipsing RMSPs (31/34, see Table 2) show radio+ $\gamma$  signals, which share the faster  $P$

( $\langle P \rangle \sim 2.78$  ms) and larger  $\dot{E}$  ( $\langle \dot{E} \rangle \sim 4.1 \times 10^{34}$ ) distributions than the non-eclipsing ones ( $\langle P \rangle \sim 4.19$  ms and  $\langle \dot{E} \rangle \sim 2.4 \times 10^{34}$ , see Table 3, Table 6, Figure 1(b) and Figure 2(b)). Since it is suggested that the eclipsing RMSPs may link to their accreting progenitors (Kluźniak et al. 1988), so we suspect that the radio+ $\gamma$  MSPs may be younger than the radio-only MSPs.

- **The  $K - S$  tests indicate that the radio+ $\gamma$  and radio-only MSPs share the different  $P$  and  $\dot{E}$  distributions (see Table 4). In addition, the  $S - W$  tests verify that the  $P$  distributions of these two MSP populations are both compatible with being log-normal (see Table 5). It should be noticed that the above conclusions depend on the sample selection introduced in section 2, however, we still suggest that there should be a physical difference between the radio+ $\gamma$  and radio-only MSPs. So far, it has been neither clear whether there is an evolutionary relation between the two MSP populations, nor what physical process dominates the difference between them, which need further observational and theoretical analysis.**

- It can be seen from Figure 1 that many accretion-powered X-ray MSPs (14/29) show the  $P$  distribution clustering around  $\sim 1.6 - 2.0$  ms, as similar to the result by Patruno et al. (2017). This phenomenon can be explained by the spinning limit due to some effect which acts as a "brake" on the NS spins, such as the gravitational wave radiation (Bildsten 1998; Andersson et al. 1999; Chakrabarty et al. 2003, 2008; Haskell & Patruno 2011; Guo et al. 2016; Patruno et al. 2017), the NS magnetic field (Patruno et al. 2012) and the transient accretion (Bhattacharyya & Chakrabarty 2017; D'Angelo 2017). However, the similar clustering phenomenon is not observed in the  $P$  distribution of RMSPs (see Figure 1). Moreover, three non-eclipsing RMSPs emitting radio+ $\gamma$  signals, i.e., PSR J0952-0607, PSR J1803+1358 and PSR J1939+2134 (B1937+21), share the even faster  $P$  of  $\sim 1.4 - 1.6$  ms (see Figure 1). It is not clear why the accretion-powered X-ray MSPs with the fast spin of  $P < 1.6$  ms, as corresponding to these three RMSPs, have not been detected (the fastest spin of the accretion-powered X-ray MSP is about 1.62 ms, see Hartman et al. 2003). We rather suggest that the clustering distribution around  $P \sim 1.6 - 2.0$  ms shown in the accretion-powered X-ray MSPs may be due to the selective effect of the limited samples.

- As an example, we take the two tMSPs in the galactic field, i.e., PSR J1023+0038 and PSR J1227-4853, as a reference to check the above results of the  $P$

and  $\dot{E}$  distributions. Firstly, the two sources are in the end phase of the accretion-powered stage with  $P \sim 1.69$  ms, which is in the clustering area around  $\sim 1.6 - 2.0$  ms shown in  $P$  distribution of the accretion-powered X-ray MSPs (see Figure 1), implying that this spin range may relate to the transitional process between the accretion- and rotation-powered stage. Moreover, the two tMSPs are the new born RMSPs with observed irregularly radio eclipses, supporting that the radio eclipsing phenomenon may link to their accreting progenitors.

The observations from multi-wavebands are critical for understanding the MSP evolution between the accretion- and rotation-powered stages, and the conclusions in this paper may provide some clues for the further investigations. In addition, the  $K - S$  test shows that RMSPs and the accretion-power X-ray MSPs share the different  $P$  distributions, implying that RMSPs is unlikely to have evolved from a single coherent progenitor population, and this fact has been noticed by Kiziltan & Thorsett (2009). Furthermore, we find that all the three observed super-fast spinning RMSPs with  $P \sim 1.4 - 1.6$  ms exhibit the non-eclipsing, so we argue that they may be the distinctive MSPs experiencing other origins, such as the accretion induced collapse of white dwarfs (Bhattacharyya & van den Heuvel 1991; Nomoto et al. 1995; Taani et al. 2012; Kiziltan et al. 2013).

**Acknowledgements** This work is supported by the National Natural Science Foundation of China (Grant No. 11703003 and No. U1731238), the Science and Technology Foundation of Guizhou Province (Grant No. [2017]5726), NAOC-Y834081V01.

## References

- Abdo, A. A., Ajello, M., Allafort, A., et al. 2013, *ApJS*, 208, 17
- Alpar, M. A., Cheng, A. F., Ruderman, M. A., & Shaham, J. 1982, *Nature*, 300, 728
- Andersson, N., Kokkotas, K. D., & Stergioulas, N. 1999, *ApJ*, 516, 307
- Archibald, A. M., Stairs, I. H., Ransom, S. M., et al. 2009, *Science*, 324, 1411
- Arons, J. 1996, *Astronomy and Astrophysics Supplement*, 120, 49
- Backer, D. C., Kulkarni, S. R., Heiles, C., Davis, M. M., & Goss, W. M. 1982, *Nature*, 300, 615
- Bassa, C. G., Patruno, A., Hessels, J. W. T., et al. 2014, *MNRAS*, 441, 1825
- Bassa, C. G., Pleunis, Z., Hessels, J. W. T., et al. 2017, *ApJL*, 846, L20
- Bhattacharya, D., & van den Heuvel, E. P. J. 1991, *Physics Reports*, 203, 1
- Bhattacharya, D., & Srinivasan, G. 1995, "The magnetic fields of neutron stars and their evolution", in "X-ray Binaries", eds. Lewin, W. H. G., van Paradijs, J., van den Heuvel, E. P. J., Cambridge University Press, Cambridge, p. 495
- Bhattacharyya, S., & Chakrabarty, D. 2017, *ApJ*, 835, 4
- Bildsten, L. 1998, *ApJ*, 501, L89
- Bilous, A. V., Watts, A. L., Galloway, D. K., & in't Zand, J. J. M. 2018, *ApJL*, 862, L4**
- Bogdanov, S., Patruno, A., Archibald, A. M., et al. 2014, *ApJ*, 789, 40
- Burderi, L., Di Salvo, T., Menna, M. T., Riggio, A., & Papitto, A. 2006, *ApJ*, 653, L133
- Burderi, L., Riggio, A., Di Salvo, T., et al. 2009, *A&A*, 496, L17
- Chakrabarty, D., Morgan, E. H., Muno, M. P., et al. 2003, *Nature*, 424, 42
- Chakrabarty, D. 2008, in *AIP Conf. Ser.* 1068, "A Decade of Accreting Millisecond X-Ray Pulsars", eds. Wijnands, R. et al., Melville, NY: AIP, p. 67
- Caraveo, P. A. 2014, *ARA&A*, 52, 211
- Clark, C. J., Pletsch, H. J., Wu, J., et al. 2018, *Science Advances*, 4, eaao7228
- D'Angelo, C. R. 2017, *MNRAS*, 470, 3316
- Di Salvo, T., Burderi, L., Riggio, A., Papitto, A., & Menna, M. T. 2008, *MNRAS*, 389, 1851
- Ferrigno, C., Bozzo, E., Papitto, A., et al. 2014, *A&A*, 567, A77
- Ferrigno, C., Bozzo, W., Sanna, A., et al. 2018, *The Astronomer's Telegram*, No. 11958**
- Fruchter, A. S., Stinebring, D. R., & Taylor, J. H. 1988, *Nature*, 333, 237
- Ghosh, P. 2007, "Rotation and Accretion Powered Pulsars", World Scientific Publishing Co., Pte. Ltd., Singapore
- Ghosh, P., & Lamb, F. K. 1979, *ApJ*, 234, 296
- Grenier, I. A., & Harding, A. K. 2015, *Comptes rendus-Physique*, 16, 641
- Guo, Y. Q., Zhang, C. M., & Pan Y. Y. 2016, *Astrophysics and Space Science*, 361, 363
- Hartman, J. M., Chakrabarty, D., Galloway, D. K., et al. 2003, *Bulletin of the American Astronomical Society*, 35, 865
- Hartman, J. M., Patruno, A., Chakrabarty, D., et al. 2008, *ApJ*, 675, 1468
- Hartman, J. M., Patruno, A., & Chakrabarty, D., et al. 2009, *ApJ*, 702, 1673
- Haskell, B., & Patruno, A. 2011, *ApJL*, 738, L14
- Hessels, J. W. T., Ransom, S. M., Stairs, I. H., et al. 2006, *Science*, 311, 1901
- Kiziltan, B., & Thorsett, S. E. 2009, *ApJ*, 693, L109
- Kiziltan, B., Kottas, A., De Yoreo, M., & Thorsett, S. E. 2013, *ApJ*, 778, 66
- Kluźniak, W., Ruderman, M., Shaham, J., & Tavani, M. 1988, *Nature*, 334, 225
- Kluźniak, W., & Rappaport, S. 2007, *ApJ*, 671, 1990
- Linares, M., Bahramian, A., Heinke, C., et al. 2014, *MNRAS*, 438, 251
- Lorimer, D. R. 2008, *Living Reviews in Relativity*, 11, 8
- Lorimer, D. R., Esposito, P., Manchester, R. N., et al. 2015, *MNRAS*, 450, 2185**
- Manchester, R. N., Hobbs, G. B., Teoh, A., & Hobbs, M. 2005, *AJ*, 129, 1993
- Nomoto, K., Iwamoto, K., Yamaoka, H., & Hashimoto, M. 1995, in *ASP Conf. Ser.* 72, *Millisecond Pulsars: A Decade of Surprise*, eds. Fruchter, A. S., Tavani, M., & Backer D. C. (San Francisco, CA: ASP), 164
- Pan, Y. Y., Song, L. M., Zhang, C. M., & Guo, Y. Q. 2015, *Astronomische Nachrichten*, 336, 370
- Patruno, A., & Watts, A. L. 2012, *arXiv:1206.2727*
- Patruno, A., Haskell, B., & D'Angelo, C. 2012, *ApJ*, 746, 9
- Patruno, A., Archibald, A. M., Hessels, J. W. T., et al. 2014, *ApJL*, 781, L3
- Patruno, A., Haskell, B., & Andersson, N. 2017, *ApJ*, 850, 106
- Papitto, A., Ferrigno, C., Bozzo, E., et al. 2013, *Nature*, 501, 517
- Papitto, A., Torres, D. F., Rea, N., & Tauris, T. M. 2014, *A&A*, 566, A64
- Papitto, A. 2016, *Memorie della Societa Astronomica Italiana*, 87, 543
- Pallanca, C., Dalessandro, E., Ferraro, F. R., Lanzoni, B., & Beccari, G. 2013, *ApJ*, 773, 122
- Ray, P. S., Abdo, A. A., Parent D., et al. 2012., in *Proc. 2011 Fermi Symp.*, Rome, Italy, May 9-12, *eConf C110509*, *arXiv:1205.3089*
- Radhakrishnan, V., & Srinivasan, G. 1982, *Current Science.*, 51, 1096
- Roberts, M. S. E. 2013, in *IAU Symp.* 291, "Neutron Stars and Pulsars: Challenges and Opportunities after 80 Years", ed. van Leeuwen, J., Cambridge Univ. Press, Cambridge, p. 127
- Roy, J., Bhattacharyya, B., & Ray, P. S. 2014, *The Astronomer's Telegram*, No. 5890
- Sanna, A., Di Salvo, T., Burderi, L., et al. 2017, *MNRAS*, 471, 463
- Sanna, A., Ferrigno, C., Ray, P. S., et al. 2018, *arXiv:1808.10195***
- Stappers, B. W., Archibald, A. M., Hessels, J. W. T., et al. 2014, *ApJ*, 790, 39
- Strohmayer, T. E., Zhang, W., Swank, J. H., et al., 1996, *ApJL*, 469, L9



- Strohmayer, T., & Bildsten, L. 2006, "New views of thermonuclear bursts", in "Compact Stellar X-Ray Sources", eds. Lewin, W. H. G., van der Klis, M., Cambridge Univ. Press, Cambridge, p. 113
- Taani, A., Zhang, C. M., Al-Wardat, M., & Zhao, Y. H. 2012, *Astrophysics and Space Science*, 340, 147
- Tauris, T. M. 2012, *Science*, 335, 561
- Torres, D. F., Ji, L., Li, J., et al. 2017, *ApJ*, 836, 68
- Watts, A. L. 2012, *ARA&A*, 50, 609
- Wijnands, R., & van der Klis, M. 1998, *Nature*, 394, 344
- Zhang, C. M., & Kojima, Y. 2006, *MNRAS*, 366, 137
- Zhang C. M., 2016, "Evolution of the Magnetic Field of Neutron Stars", in "Handbook of Supernovae", eds. Alsabti A. W. & Murdin P., Springer International Publishing AG
- Zhang, C. M., Wang, J., Zhao, Y. H., et al. 2011, *A&A*, 527, A83